

A Critical Role for the PAR-1/MARK-tau Axis in Mediating the Toxic Effects of A β on Synapses and Dendritic Spines

Journal:	<i>Human Molecular Genetics</i>
Manuscript ID:	HMG-2011-W-01229.R1
Manuscript Type:	1 General Article - US Office
Date Submitted by the Author:	30-Nov-2011
Complete List of Authors:	Yu, Wendou; Stanford University, Pathology Polepalli, Jai; Stanford University, Psychiatry and Behavioral Science Wagh, Dhananjay; Stanford University, Neurology Rajadas, Jayakumar; Stanford University, Neurology Malenka, Rob; Stanford University, Psychiatry Lu, Bingwei; Stanford University, Pathology
Key Words:	Amyloid-beta, tau, PAR-1/MARK, Synapse , Dendritic spines

1
2
3
4
5
6
7
8
9
10
11
12
13
14
15
16
17
18
19
20
21
22
23
24
25
26
27
28
29
30
31
32
33
34
35
36
37
38
39
40
41
42
43
44
45
46
47
48
49
50
51
52
53
54
55
56
57
58
59
60

A Critical Role for the PAR-1/MARK-tau Axis in Mediating the Toxic Effects of A β on Synapses and Dendritic Spines

Wendou Yu¹, Jai Polepalli², [Dhananjay Wagh](#)³, Jayakumar Rajadas³, Robert Malenka²,
Bingwei Lu^{1*}

¹Department of Pathology

²Department of Psychiatry and Behavioral Science

³Biomaterial and Advanced Drug Delivery Laboratory

Stanford University School of Medicine, Stanford, CA 94305, USA

*Corresponding author:

Bingwei Lu, Department of Pathology, Stanford University School of Medicine, R270

Edwards Building, Stanford, CA 94305

Phone: 650 723-1828

Fax: 650 498-6616

email: bingwei@stanford.edu

ABSTRACT

Alzheimer's disease (AD) is the most common neurodegenerative disease and the leading cause of dementia in the elderly. Accumulating evidence support soluble amyloid- β ($A\beta$) oligomers as the leading candidate for the causative agent in AD and synapses as the primary site of $A\beta$ oligomer action. However, the molecular and cellular mechanisms by which $A\beta$ oligomers cause synaptic dysfunction and cognitive impairments remain poorly understood. Using primary cultures of rat hippocampal neurons as a model system, we show that the **PAR-1/MARK family kinases act as critical mediators** of $A\beta$ toxicity on synapses and dendritic spines. Overexpression of **MARK4** led to tau hyperphosphorylation, reduced expression of synaptic markers, and loss of dendritic spines and synapses, phenotypes also observed after $A\beta$ treatment. Importantly, expression of a non-phosphorylatable form of tau with the PAR-1/MARK site mutated blocked the synaptic toxicity induced by **MARK4** overexpression or $A\beta$ treatment. To probe the involvement of endogenous **MARK kinases** in mediating the synaptic toxicity of $A\beta$, we employed a peptide inhibitor capable of effectively and specifically inhibiting the activities of all PAR-1/MARK family members. This inhibitor abrogated the toxic effects of $A\beta$ oligomers on dendritic spines and synapses as assayed at the morphological and electrophysiological levels. Our results reveal a critical role for PAR-1/MARK kinases in AD pathogenesis and suggest PAR-1/MARK inhibitors as potential therapeutics for AD and possibly other tauopathies where aberrant tau hyperphosphorylation is involved.

INTRODUCTION

Despite the identification of amyloid plaques (AP) and neurofibrillary tangles (NFT) as pathological hallmarks of Alzheimer's disease (AD), the memory deficits in AD patients do not correlate well with AP or NFT burden; instead, loss of synaptic markers is a better predictor of clinical symptoms and disease progression, lending support to the notion that AD is a disease of synaptic failure [1]. Synapses and dendritic spines are dynamic structures whose plasticity is thought to underlie learning and memory and contribute to AD pathogenesis [2]. Accumulating evidence support that A β is the primary agent causative of synaptic and spine pathology in AD [3,4,5]. For example, rare genetic mutations cause familial AD by altering the production or metabolism of A β [6,7], the soluble pool of which correlates with disease progression and severity [5], and depletion of soluble A β in mouse AD models rescued the cognitive deficits [8]. Moreover, synthetic A β oligomers or those purified from cultured cells or brain samples can induce neuritic degeneration, neurotransmission defects, and spine loss [9,10,11,12]. The detailed cellular and biochemical mechanisms involved, however, remain poorly defined.

Recent studies have supported tau as a major mediator of A β toxicity. In mouse models, intracranial injection of A β or crossing an APP transgene into tau transgenic animals promoted NFT pathology [13,14,15], and antibody-based removal of A β reduced hyperphosphorylated tau and rescued behavioral and pathological defects in a APP/Psn/tau 3xTg AD mouse model [16]. Moreover, removal of tau relieved A β -induced neurotoxicity in culture [17], and prevented A β - induced behavioral deficits in an h-APP Tg mouse model [18]. Together, these studies support the critical involvement of tau in mediating the toxicity of A β in AD pathogenesis.

1
2
3
4
5
6
7
8
9
10
11
12
13
14
15
16
17
18
19
20
21
22
23
24
25
26
27
28
29
30
31
32
33
It is not clear how tau abnormality arises in AD. Current efforts have focused on the role of tau hyperphosphorylation [19,20]. A number of kinases and phosphatases are shown to regulate tau phosphorylation [21], but few of them have been examined for roles in linking amyloid with tau pathology. A strong case has been made for partitioning defective-1 (PAR-1)/microtubule affinity regulating kinase (MARK). PAR-1 was originally identified for its role in regulating cell polarity [22]. PAR-1 and its mammalian homologue MARK phosphorylate tau associate with NFT [23,24]. In *Drosophila* models, PAR-1-mediated phosphorylation is required for conferring tau toxicity [25]. Elevation of PAR-1/MARK-mediated tau phosphorylation (at 12E8 sites) was observed in AD patients and mouse AD models [26,27]. Activated *Drosophila* PAR-1 also directly phosphorylates the postsynaptic density protein 95 (PSD-95) homologue discs large (Dlg), impairing its postsynaptic localization [28], which might be mechanistically related to the synaptic loss of PSD-95 seen in early stages of AD in patients and mouse models [29,30].

34
35
36
37
38
39
40
41
42
43
44
45
46
47
48
49
50
51
52
53
54
55
56
57
58
59
60
The studies described above strongly implicate PAR-1/MARK kinases as critical players in AD. Consistent with this hypothesis, a recent genome-wide association study suggested a potential link of MARK4 to late onset AD [31,32], an observation requiring further validation, and PAR-1/MARK kinases are activated by APP or A β oligomers in *Drosophila* or mammalian neurons, respectively [33,34]. To more rigorously test the pathogenic role of PAR-1/MARK kinases and to validate them as potential drug target, loss-of-function analysis in mammalian systems is critically needed. However, functional redundancy among at least 4 members of the mammalian PAR-1/MARK kinase family presents a considerable challenge for a genetic loss-of-function approach. In this study, we describe a pharmacological approach using a specific peptide inhibitor to probe the

1
2
3 importance of PAR-1/MARK in mediating the synaptic and dendritic toxicity of A β in
4
5 primary cultures of rat hippocampal neurons. Our results provide compelling evidence
6
7 that PAR-1/MARK kinases are critically involved in mediating the synaptic toxicity of
8
9 A β by promoting the aberrant phosphorylation of tau and PSD-95, and that inhibition of
10
11 PAR-1/MARK kinases represent a viable therapeutic approach.
12
13
14
15
16
17

18 RESULTS

20 Overexpression of MARK4 induces defects in synapses and dendritic spines

21 We used cultured rat primary hippocampal neurons to test whether the PAR-1/MARK
22
23 family kinases mediates AD-related neurotoxicity in mammals. In addition to being the
24
25 relevant cell type for studying AD pathogenesis, these neurons offer excellent cellular
26
27 resolution for studying synaptic and dendritic spine morphologies and for
28
29 electrophysiological characterization. As expected, we found that overexpression of
30
31 *Drosophila* PAR-1 or mammalian MARK4 [31] in hippocampal neurons resulted in
32
33 hyperphosphorylation of tau at the phosphorylation sites recognized by the 12E8
34
35 antibody (Supplementary Material, Figure S1), sites known to be phosphorylated by
36
37 PAR-1/MARK [23,25]. This was accompanied by a number of phenotypes including loss
38
39 of dendritic spines (Fig. 1A-C, F), the delocalization of PSD-95 from synapses (Fig. 1A,
40
41 F), and decreased expression of other synaptic markers such as GluR1, a subunit of α -
42
43 amino-3-hydroxy-5-methyl-4-isoxazolepropionic acid (AMPA) receptors (Fig. 1B, F),
44
45 and the presynaptic protein Synapsin I (Fig. 1C, F). In addition, we also observed defects
46
47 in mitochondria localization in PAR-1 or MARK4 overexpressing neurons (data not
48
49 shown). The kinase-dead form of MARK4 (MARK4-KD) had no such effect, indicating
50
51
52
53
54
55
56
57
58
59
60

1
2
3 that kinase activity is required for inducing the observed toxic effects. Both MARK4-WT
4 and MARK4-KD exhibited relatively uniform distribution in the dendrites (Fig. 1A-C,
5
6 green signals).
7
8
9

10 Previous studies in *Drosophila* showed that PAR-1 could regulate the postsynaptic
11 localization of Dlg through direct phosphorylation [28]. The phosphorylation site is
12 conserved in PSD-95, the mammalian homologue of Dlg. To test whether MARK4 may
13 directly act on PSD-95 to regulate its synaptic localization, we generated a mutant form
14 of PSD-95 in which the conserved PAR-1/MARK target site is mutated to Ala (PSD-95-
15 SA). Both the WT and SA mutant forms of PSD-95 were fused with GFP to facilitate
16 visualization. In the same expression vector, shRNAs targeting endogenous PSD-95 but
17 not the exogenous PSD-95-GFP were also expressed [35]. Thus the observed effects were
18 largely free of potential interference from endogenous PSD-95. While PSD-95-WT-EGFP
19 was delocalized from the dendritic spines by MARK4 and was present uniformly in the
20 dendritic shaft, PSD-95-SA-EGFP effectively resisted the effect of MARK4 and
21 maintained its punctate synaptic localization (Fig. 1D, G), consistent with MARK4
22 directly regulating PSD-95 localization in mammalian hippocampal neurons through
23 phosphorylation.
24
25
26
27
28
29
30
31
32
33
34
35
36
37
38
39
40
41
42
43
44
45

46 **Expression of a non-phosphorylatable form of tau blocks PAR-1/MARK toxicity**

47 We were interested in identifying the key substrates through which PAR-1/MARK
48 **overexpression** leads to synaptic and dendritic spine toxicity. Previous studies showed
49 that PAR-1 overexpression in *Drosophila* photoreceptors caused neurotoxicity through
50 phosphorylation of tau in the microtubule-binding domain, and that a mutant form of tau
51
52
53
54
55
56
57
58
59
60

1
2
3 with the PAR-1 site mutated (tauS2A) not only was itself non-toxic but also could block
4 PAR-1 overexpression-induced neurotoxicity [25]. Co-transfection of a similar
5
6 phosphorylation-mutant form of tau (h-tau-SA) blocked the toxic effects of MARK4 in
7
8 rat hippocampal neurons, including the spine loss, whereas wild type human tau (h-tau-
9
10 WT) failed to do so (Fig. 1E, G). This is consistent with tau being a major mediator of
11
12
13
14
15 MARK4 toxicity on synapses and dendritic spines.
16
17

18 19 20 **Expression of non-phosphorylatable form of tau blocks A β toxicity**

21
22 We further tested whether phosphorylation of tau by MARK might mediate the toxicity of
23
24 A β on neuronal synapses and dendritic spines. Although MARK activation and elevation
25
26 of tau phosphorylation at PAR-1/MARK target sites occurred in hippocampal neurons
27
28 after A β oligomer treatment [11,34], it is not clear whether these events were disease-
29
30 causing or simply a compensatory, protective response. Indeed, overexpression of
31
32 MARK2 was reported to be able to rescue tau-induced synapse and spine loss [36].
33
34 Consistent with previous reports [11,34], treatment of rat hippocampal neurons with
35
36 synthetic A β , prepared using a well-characterized procedure that enriches for
37
38 A β oligomers [37], resulted in increased tau phosphorylation at the 12E8 sites (Fig. 2A),
39
40 suggesting that A β treatment had activated **MARK kinases**. Increased phosphorylation of
41
42 tau at a site recognized by the PHF-1 phospho-tau antibody was also observed (data not
43
44 shown). A β treatment also caused losses of synaptic marker expression and dendritic
45
46 spines as seen in the PAR-1/MARK overexpression condition (Fig. 2B-E, G). Strikingly,
47
48 in neurons transfected with h-tau-S2A but not h-tau-WT, the toxic effect of A β in causing
49
50 spine loss was ameliorated (Fig. 2F, G). The toxic effects of A β on the density of synaptic
51
52
53
54
55
56
57
58
59
60

1
2
3 marker PSD-95 and GluR1 clusters were also rescued by h-tau-S2A (Fig. 2H). These
4
5 results support the notion that phosphorylation of tau by PAR-1/MARK family kinases is
6
7 a primary downstream event by which A β exerts its toxicity on hippocampal synapses
8
9 and dendritic spines.
10
11

12 13 14 15 16 **A PAR-1/MARK inhibitor effectively blocked A β toxicity**

17
18 Next we wished to assess the involvement of endogenous MARK kinases in mediating
19
20 A β toxicity. To circumvent potential functional redundancy among at least 4 mammalian
21
22 MARK family members, we used a peptide inhibitor (MKI) derived from the CagA
23
24 protein of *Helicobacter pylori*, which can specifically bind with high affinity to the
25
26 substrate-binding sites of all MARKs by mimicking the natural substrates of these
27
28 kinases [38]. We first confirmed that expression of a MKI-GFP fusion protein in rat
29
30 hippocampal neurons effectively attenuated MARK4-mediated phosphorylation of both
31
32 endogenous tau (Fig. 3A) and transfected human tau at the 12E8 sites (Fig. 3B).
33
34 Phosphorylation of tau at the PHF-1 site was also reduced by MKI (Fig. 3A). It is
35
36 possible that the PHF-1 site is also targeted by PAR-1/MARKs *in vivo*, or that the
37
38 phosphorylation of tau at the 12E8 sites is a prerequisite for PHF-1 site phosphorylation,
39
40 as the 12E8 sites were previously shown to be required for tau phosphorylation at other
41
42 sites [25]. Supporting the specificity of the MKI effect on PAR-1/MARK, under similar
43
44 experimental conditions MKI-EGFP did not affect the phosphorylation of acetyl-CoA
45
46 carboxylase (ACC) by AMP activated kinase (AMPK) (Fig. 3C), which is closely related
47
48 to PAR-1/MARK on the protein kinase phylogenetic tree [39]. MARK4 overexpression-
49
50
51
52
53
54
55
56
57
58
59
60

1
2
3 induced synaptic defects including spine loss (Fig. 3D, E) and reduction of PSD-95 and
4
5 GluR1 puncta density were all effectively blocked by MKI-EGFP (Fig. 3E).
6
7

8 To test the function of **MARK kinases** in mediating the toxicity of A β on synapses
9
10 and dendritic spines, we next examine the effect of MKI in modulating the toxicity of A β .
11
12 Remarkably, MKI-GFP expression effectively blocked the morphological defects caused
13
14 by A β , such as the loss of dendritic spines (Fig. 4A-C), and the reduction in the density of
15
16 PSD-95 (Fig. 4A, C) and GluR1 puncta (Fig. 4B, C).
17
18

19
20 We further examined the effect of MKI-EGFP at the functional level by
21
22 performing electrophysiological analysis. A β treatment caused a reduction in the
23
24 frequency but not amplitude of AMPAR-mediated miniature excitatory postsynaptic
25
26 current (mEPSC) (Fig. 4D). The reduction in the mEPSC frequency suggested that A β is
27
28 causing a reduction in synapse number, whereas the unchanged mEPSC amplitude
29
30 indicated that the postsynaptic AMPA receptor composition and/or activity of the
31
32 remaining synapses were probably not affected. The reduction of mEPSC frequency
33
34 caused by A β was effectively rescued by MKI-EGFP (Fig. 4D). **We note that neurons**
35
36 **expressing MKI-EGFP alone also showed reduced mEPSC frequency but not amplitude**
37
38 **(Fig. 4D), suggesting that the PAR-1/MARK family kinases have a normal physiological**
39
40 **function in hippocampal neurons and that its appropriate level is important for synaptic**
41
42 **function.**
43
44
45
46
47
48
49
50

51 **DISCUSSION**

52
53 The amyloid and tau lesions are pathological hallmarks of AD that are present in virtually
54
55 all AD cases. The relationship between the two, however, remains unresolved.
56
57
58
59
60

1
2
3 Accumulating evidence support the toxic oligomers formed by the A β peptide as the
4 disease-causing agents, and synapses and dendritic spines as their major sites of action.
5
6 Here we show that A β acts through the PAR-1/MARK family kinases to impinge on tau
7
8 to affect synaptic function and dendritic spine morphogenesis. This conclusion is
9
10 supported by the suppression of A β toxicity by either the co-expression of a phospho-
11
12 mutant form of tau that can no longer be phosphorylated by PAR-1/MARK, or the
13
14 specific inhibition of PAR-1/MARK with a peptide inhibitor. Our findings are consistent
15
16 with the hypothesis that tau abnormality is a major downstream pathogenic event in the
17
18 signaling cascade initiated by A β [6], and the observation that removal of endogenous tau
19
20 attenuates learning and memory deficits in AD models [18].
21
22
23
24
25
26

27
28 One major question concerns how tau abnormality, specifically its
29
30 hyperphosphorylation, leads to synaptic and dendritic spine pathology. Despite tau being
31
32 best known as an axonal protein, phospho-tau was shown to accumulate in dendritic
33
34 spines, where it may affect the synaptic trafficking and/or anchoring of glutamate
35
36 receptors, thereby influencing postsynaptic function [40]. It is not clear whether phospho-
37
38 tau is being actively transported to the dendritic compartment, or that due to its
39
40 compromised ability to bind microtubules, especially after being phosphorylated by PAR-
41
42 1/MARK, phospho-tau simply diffuses from axon to other cellular compartments.
43
44 Dendritic tau was recently found to recruit fyn kinase, facilitating fyn-mediated
45
46 phosphorylation of GluR2 and stabilizing the interaction between GluR2 and PSD-95
47
48 [41]. This potentially promotes excitotoxicity and represents a possible mechanism by
49
50 which dendritic tau mediates A β toxicity. It remains to be determined whether dendritic
51
52 tau has a normal physiological function. Since A β -induced spine loss was preventable by
53
54
55
56
57
58
59
60

1
2
3 taxol [34], tau-related microtubule destabilization and trafficking defects may also
4
5 mediate A β toxicity.
6
7

8
9
10 Much of the molecular events linking A β to tau pathologies remain to be
11 elucidated. The implication of PAR-1/MARK in this process offers a new entry point to
12 further dissect the signaling process. Several kinases have been shown to act upstream of
13 PAR-1/MARK [42], including LKB1 [33]. It would be interesting to test the involvement
14
15 of these kinases in mediating A β toxicity through regulation of PAR-1/MARK. Previous
16
17 studies have indicated that tau phosphorylation at the PAR-1/MARK target sites also
18
19 respond to other stress stimuli including osmotic stress, oxidative stress, serum
20
21 deprivation, and glutamate-induced excitotoxicity [33,34], suggesting that other triggers
22
23 of the disease may also impinge on the PAR-1/MARK-tau axis. A β could also induce
24
25 reversible synapse loss by modulating an NMDA-type GluR-dependent signaling
26
27 pathway [43], or use long-term depression (LTD)-related signaling mechanisms to affect
28
29 synaptic function and dendritic spine morphology [44]. Whether these signaling
30
31 pathways are connected to the PAR-1/MARK-tau axis will be important future research
32
33 directions. It also remains to be determined whether A β oligomers act by directly
34
35 activating transmembrane receptors, changing neuronal membrane properties, or simply
36
37 by causing cellular stress [4,34].
38
39
40
41
42
43
44
45

46
47 Our results suggest that targeting PAR-1/MARK kinases represent a potential
48
49 strategy to prevent the synaptic toxicity of A β , thereby preventing or treating the synaptic
50
51 defects of AD. *In vivo* studies applying MKI to various AD mouse models with clear
52
53 learning and memory deficits are needed to validate this therapeutic approach. One major
54
55 concern is the potential side effects, given the myriad cellular functions of PAR-1/MARK
56
57
58
59
60

1
2
3 kinases [42]. This concern is warranted by our observation that although MKI restored
4 normal neurotransmission to A β oligomer-treated neurons, it led to reduced mEPSC
5 frequency in mock-treated neurons, suggesting that appropriate levels of PAR-1/MARK
6 activity is important for neurotransmission. Thus, in A β oligomer-treated neurons, which
7 possess elevated PAR-1/MARK activity [34], MKI tuned down kinase activity to a level
8 compatible with normal neurotransmission. However, in normal neurons, reduction of
9 PAR-1/MARK activity by MKI to below threshold levels could compromise
10 neurotransmission. It will therefore be necessary to adjust MKI dosages to achieve
11 therapeutic effect without causing serious side effects. The same could be said for
12 therapeutic approaches targeting A β or tau. For example, the production of A β is
13 positively regulated by neuronal activity [45], and A β can in turn depress excitatory
14 synaptic transmission [46]. This negative feedback regulatory loop may normally serve to
15 restrain neuronal hyperactivity, such that therapeutic approaches leading to too much
16 removal of A β might have unwanted side effects as well.
17
18
19
20
21
22
23
24
25
26
27
28
29
30
31
32
33
34
35
36
37
38
39

40 MATERIALS AND METHODS

41 Hippocampal neuronal culture and transfection

42
43 Rat E18 hippocampal neuron primary cultures were prepared as described [47]. Cultured
44 neurons (10-day *in vitro*) in 12-well plates were transfected with 2–3 μ g of plasmid/well
45 using a CalPhos Mammalian Transfection Kit (Clontech, San Jose, CA, USA).
46
47
48
49
50

51
52 Fluorescence immunocytochemistry was performed 3 days after transfection. Preparation
53 and concentration of lentiviral particles were performed as described before [47]. Viral
54 transfection of hippocampal neurons was carried out at 10 days after *in vitro* culture. The
55
56
57
58
59
60

1
2
3 next day, culture medium was replaced with 50% fresh medium plus 50% conditioned
4
5 medium.
6
7

10 **A β oligomer preparation**

11 Commercial A β -42 peptide was purchased from rPeptide (Bogart, GA, USA). A β
12
13 oligomer was prepared following a published protocol [37]. Briefly, A β -42 was dissolved
14
15 in hexafluoroisopropanol (HFIP) at 4 $\mu\text{g}/\mu\text{l}$ and aliquoted into 0.6 ml tubes. Peptide films
16
17 were obtained by evaporating HFIP with a Speed VAC and stored at -80°C . Prior to use,
18
19 the peptide was dissolved in phosphate buffer (pH7.4) to 80 μM and incubated at 4°C for
20
21 24 h. Culture medium containing 5 μM A β were used to treat neurons.
22
23
24
25
26
27
28
29

30 **Recombinant DNA construction**

31
32 EGFP-tagged PSD-95-WT in the FHUGW lentivirus vector was described before [35].
33
34 The S561A mutation was introduced by site-directed mutagenesis. Tau S2A mutations
35
36 were introduced as described before [25], and subcloned into FHUGW with a C-terminal
37
38 HA tag. EGFP- and HA-tagged human MARK4 constructs were obtained from Dr.
39
40 Gerard Drewes. MKI cDNA was obtained from Dr. C. Erec Stebbins, and subcloned into
41
42 FHUGW vector with a C-terminal EGFP tag.
43
44
45
46
47
48

49 **Immunofluorescence analysis**

50
51 Chicken anti-EGFP (1:4000) and rabbit anti-HA (1:3000) antibodies were purchased
52
53 from Abcam (Cambridge, MA, USA); Mouse anti-Myc (1:1500, 4A6) and mouse anti-
54
55 PSD-95 (1:300) from Millipore (Billerica, MA, USA); Rabbit anti-GluR1 (1:200) from
56
57
58
59
60

1
2
3 Calbiochem (San Diego, CA), and Rabbit anti-Synapsin I (1: 1000) from Sigma (St Louis,
4 MO, USA). Immunofluorescence analysis was done essentially as described before [47].
5
6
7
8 Confocal images were obtained using a Leica TCS SP5 confocal microscope or Zeiss
9
10 inverted LSM510 confocal microscope (Carl Zeiss, Inc.) with 63× NA 1.4 objectives.
11
12 Processed confocal images were used to make 2D projections. Dendritic spine number
13
14 and clusters of PSD-95, GluR1, or Synapsin I were manually counted as the number
15
16 along a 10µm length of dendrite and presented as mean ± SEM. Each experiment has
17
18 been done at least three times and 6–9 neurons were randomly selected for analysis each
19
20 time. Between 15-30 dendritic processes were selected for quantification. Data were
21
22 analyzed while blind to the conditions.
23
24
25
26
27
28

29 **Electrophysiology in dissociated cultures**

30
31 Whole-cell patch-clamp recordings were made from neurons at 13-14 DIV in voltage
32
33 clamp mode using a Multiclamp 700B amplifier (Molecular Devices, Union City, CA),
34
35 digitized at 10 kHz and filtered at 4 kHz. Data was acquired and analyzed using
36
37 AxographX (Axograph, Sydney). Whole-cell recording pipettes (3-5 MΩ) were filled
38
39 with a solution containing (in mM) 135 CsMeSO₄, 8 NaCl, 10 HEPES, 0.25 EGTA, 2
40
41 Mg₂ATP, 0.3 Na₃GTP, 0.1 spermine and 7 phosphocreatine. The bath solution contained
42
43 (in mM): 140 NaCl, 2.5 KCl, 2 CaCl₂, 2 MgCl₂, 10 HEPES-NaOH pH 7.4 and 10 glucose.
44
45
46 Miniature AMPAR-mediated EPSCs were isolated by including D-APV (50 µM),
47
48 picrotoxin (100 µM), and 1 µM tetrodotoxin in the bath solution. All recordings were
49
50 performed at a holding potential of -70 mV at room temperature. mEPSCs were identified
51
52 using a template with a threshold of -6pA (2.5 x SD of the noise), and were individually
53
54
55
56
57
58
59
60

1
2
3 proofread for accuracy. To plot summary graphs, average frequency from the EGFP
4
5 control cells from each culture preparation was normalized. Individual cells from all four
6
7 conditions were then compared to this normalized average.
8
9

10 11 12 **CONFLICT OF INTEREST STATEMENT:**

13
14
15 The authors declare that there is no conflict of interest.
16
17

18 19 20 **FUNDING**

21
22 This project is supported by Dean's Postdoctoral Fellowship, Stanford University School
23
24 of Medicine (WY), Brain Disorders Award from the McKnight Endowment Fund for
25
26 Neurosciences (BL), and National Institute of Health grants R01MH080378 (BL),
27
28 R01AR054926 (BL), and R01MH063394 (RM).
29
30
31
32
33

34 35 **ACKNOWLEDGEMENTS**

36 We thank Drs. Gerard Drewes and C. Erec Stebbins for reagents, Dr. Su Guo for reading
37
38 the manuscript, and members of the Lu and Malenka Laboratories for discussions.
39
40
41
42

43 44 **REFERENCES**

- 45
46 1. Selkoe, D.J. (2002) Alzheimer's disease is a synaptic failure. *Science*, 298, 789-
47
48 791.
49
50 2. Penzes, P., Cahill, M.E., Jones, K.A., VanLeeuwen, J.E., and Woolfrey, K.M.
51
52 (2011) Dendritic spine pathology in neuropsychiatric disorders. *Nat. Neurosci.*, **14**,
53
54 285-293.
55
56
57
58
59
60

- 1
2
3 3. Spires, T.L., Meyer-Luehmann, M., Stern, E.A., McLean, P.J., Skoch, J. et al.
4
5 (2005) Dendritic spine abnormalities in amyloid precursor protein transgenic mice
6
7 demonstrated by gene transfer and intravital multiphoton microscopy. *J. Neurosci.*,
8
9 **25**, 7278-7287.
10
- 11
12 4. Reddy, P.H., and Beal, M.F. (2008) Amyloid beta, mitochondrial dysfunction and
13
14 synaptic damage: implications for cognitive decline in aging and Alzheimer's
15
16 disease. *Trend. Mol. Med.*, **14**, 45-53.
17
- 18
19 5. Selkoe DJ (2008) Soluble oligomers of the amyloid beta-protein impair synaptic
20
21 plasticity and behavior. *Behav. Brain Res.*, **192**, 106-113.
22
23
- 24
25 6. Hardy, J., and Selkoe, D.J. (2002) The amyloid hypothesis of Alzheimer's disease:
26
27 progress and problems on the road to therapeutics. *Science*, **297**, 353-356.
28
- 29
30 7. Holtzman, D.M., Morris, J.C., and Goate, A.M. (2011) Alzheimer's disease: the
31
32 challenge of the second century. *Sci. Transl. Med.*, **3**, 77sr71.
33
- 34
35 8. Billings, L.M., Oddo, S., Green, K.N., McGaugh, J.L., and LaFerla, F.M. (2005)
36
37 Intraneuronal Abeta causes the onset of early Alzheimer's disease-related
38
39 cognitive deficits in transgenic mice. *Neuron*, **45**, 675-688.
40
- 41
42 9. Yankner, B.A., Dawes, L.R., Fisher, S., Villa-Komaroff, L., Oster-Granite, M.L. et
43
44 al. (1989) Neurotoxicity of a fragment of the amyloid precursor associated with
45
46 Alzheimer's disease. *Science*, **245**, 417-420.
47
- 48
49 10. Walsh DM, Klyubin I, Fadeeva JV, Cullen WK, Anwyl R, et al. (2002) Naturally
50
51 secreted oligomers of amyloid beta protein potently inhibit hippocampal long-
52
53 term potentiation in vivo. *Nature*, **416**, 535-539.
54
55
56
57
58
59
60

- 1
2
3 11. Jin, M., Shepardson, N., Yang, T., Chen, G., Walsh, D. et al. (2011) Soluble
4 amyloid beta-protein dimers isolated from Alzheimer cortex directly induce Tau
5 hyperphosphorylation and neuritic degeneration. *Proc. Natl. Acad. Sci. USA*, **108**,
6 5819-5824.
7
- 8
9 12. Lambert, M.P., Barlow, A.K., Chromy, B.A., Edwards, C., Freed, R. et al. (1998)
10 Diffusible, nonfibrillar ligands derived from Abeta1-42 are potent central nervous
11 system neurotoxins. *Proc. Natl. Acad. Sci. USA*, **95**, 6448-6453.
12
- 13 13. Lewis, J., Dickson, D.W., Lin, W.L., Chisholm, L., Corral, A. et al. (2001)
14 Enhanced neurofibrillary degeneration in transgenic mice expressing mutant tau
15 and APP. *Science*, **293**, 1487-1491.
16
- 17 14. Gotz, J., Chen, F., van Dorpe, J., and Nitsch, R.M. (2001) Formation of
18 neurofibrillary tangles in P3011 tau transgenic mice induced by Abeta 42 fibrils.
19 *Science*, **293**, 1491-1495.
20
- 21 15. Oddo, S., Caccamo, A., Shepherd, J.D., Murphy, M.P., Golde, T.E. et al. (2003)
22 Triple-transgenic model of Alzheimer's disease with plaques and tangles:
23 intracellular Abeta and synaptic dysfunction. *Neuron*, **39**, 409-421.
24
- 25 16. Oddo, S., Billings, L., Kesslak, J.P., Cribbs, D.H., and LaFerla, F.M. (2004) Abeta
26 immunotherapy leads to clearance of early, but not late, hyperphosphorylated tau
27 aggregates via the proteasome. *Neuron*, **43**, 321-332.
28
- 29 17. Rapoport, M., Dawson, H.N., Binder, L.I., Vitek, M.P., and Ferreira, A. (2002)
30 Tau is essential to beta -amyloid-induced neurotoxicity. *Proc. Natl. Acad. Sci.*
31 *USA*, **99**, 6364-6369.
32
33
34
35
36
37
38
39
40
41
42
43
44
45
46
47
48
49
50
51
52
53
54
55
56
57
58
59
60

- 1
2
3
4
5
6
7
8
9
10
11
12
13
14
15
16
17
18
19
20
21
22
23
24
25
26
27
28
29
30
31
32
33
34
35
36
37
38
39
40
41
42
43
44
45
46
47
48
49
50
51
52
53
54
55
56
57
58
59
60
18. Roberson, E.D., Scarce-Levie, K., Palop, J.J., Yan, F., Cheng, I.H. et al. (2007) Reducing endogenous tau ameliorates amyloid beta-induced deficits in an Alzheimer's disease mouse model. *Science*, **316**, 750-754.
 19. Spires-Jones, T.L., Stoothoff, W.H., de Calignon, A., Jones, P.B., and Hyman, B.T. (2009) Tau pathophysiology in neurodegeneration: a tangled issue. *Trend. Neurosci.*, **32**, 150-159.
 20. Ittner, L.M., and Gotz, J. (2011) Amyloid-beta and tau--a toxic pas de deux in Alzheimer's disease. *Nat. Rev. Neurosci.*, **12**, 65-72.
 21. Lee, V.M., Goedert, M., and Trojanowski, J.Q. (2001) Neurodegenerative tauopathies. *Annu. Rev. Neurosci.* **24**, 1121-1159.
 22. Guo, S., and Kemphues, K.J. (1995) par-1, a gene required for establishing polarity in *C. elegans* embryos, encodes a putative Ser/Thr kinase that is asymmetrically distributed. *Cell*, **81**, 611-620.
 23. Drewes, G., Ebner, A., Preuss, U., Mandelkow, E.M., and Mandelkow, E. (1997) MARK, a novel family of protein kinases that phosphorylate microtubule-associated proteins and trigger microtubule disruption. *Cell*, **89**, 297-308.
 24. Chin, J.Y., Knowles, R.B., Schneider, A., Drewes, G., Mandelkow, E.M. et al. (2000) Microtubule-affinity regulating kinase (MARK) is tightly associated with neurofibrillary tangles in Alzheimer brain: a fluorescence resonance energy transfer study. *J. Neuropathol. Exp. Neurol.*, **59**, 966-971.
 25. Nishimura, I., Yang, Y., and Lu, B. (2004) PAR-1 kinase plays an initiator role in a temporally ordered phosphorylation process that confers tau toxicity in *Drosophila*. *Cell*, **116**, 671-682.

- 1
2
3
4 26. Augustinack, J.C., Schneider, A., Mandelkow, E.M., and Hyman, B.T. (2002)
5
6 Specific tau phosphorylation sites correlate with severity of neuronal
7
8 cytopathology in Alzheimer's disease. *Acta. Neuropathol.*, **103**, 26-35.
9
- 10
11 27. Perez, M., Ribe, E., Rubio, A., Lim, F., Moran, M.A. et al. (2005)
12
13 Characterization of a double (amyloid precursor protein-tau) transgenic: tau
14
15 phosphorylation and aggregation. *Neuroscience*, **130**, 339-347.
16
- 17
18 28. Zhang, Y., Guo, H., Kwan, H., Wang, J.W., Kosek, J. et al. (2007) PAR-1 kinase
19
20 phosphorylates Dlg and regulates its postsynaptic targeting at the Drosophila
21
22 neuromuscular junction. *Neuron*, **53**, 201-215.
23
- 24
25 29. Gyllys, K.H., Fein, J.A., Yang, F., Wiley, D.J., Miller, C.A. et al. (2004) Synaptic
26
27 changes in Alzheimer's disease: increased amyloid-beta and gliosis in surviving
28
29 terminals is accompanied by decreased PSD-95 fluorescence. *Am. J. Pathol.*, **165**,
30
31 1809-1817.
32
- 33
34 30. Almeida, C.G., Tampellini, D., Takahashi, R.H., Greengard, P., Lin, M.T. et al.
35
36 (2005) Beta-amyloid accumulation in APP mutant neurons reduces PSD-95 and
37
38 GluR1 in synapses. *Neurobiol. Dis.*, **20**, 187-198.
39
- 40
41 31. Trinczek, B., Brajenovic, M., Ebnet, A., and Drewes G (2004) MARK4 is a
42
43 novel microtubule-associated proteins/microtubule affinity-regulating kinase that
44
45 binds to the cellular microtubule network and to centrosomes. *J. Biol. Chem.*, **279**,
46
47 5915-5923.
48
49
- 50
51 32. Seshadri, S., Fitzpatrick, A.L., Ikram, M.A., DeStefano, A.L., Gudnason, V. et al.
52
53 (2010) Genome-wide analysis of genetic loci associated with Alzheimer disease.
54
55 *JAMA*, **303**, 1832-1840.
56
57
58
59
60

- 1
2
3
4
5
6
7
8
9
10
11
12
13
14
15
16
17
18
19
20
21
22
23
24
25
26
27
28
29
30
31
32
33
34
35
36
37
38
39
40
41
42
43
44
45
46
47
48
49
50
51
52
53
54
55
56
57
58
59
60
33. Wang, J.W., Imai, Y., and Lu, B. (2007) Activation of PAR-1 kinase and stimulation of tau phosphorylation by diverse signals require the tumor suppressor protein LKB1. *J. Neurosci.*, **27**, 574-581.
34. Zempel, H., Thies, E., Mandelkow, E., and Mandelkow, E.M. (2010) Abeta oligomers cause localized Ca(2+) elevation, missorting of endogenous Tau into dendrites, Tau phosphorylation, and destruction of microtubules and spines. *J. Neurosci.*, **30**, 11938-11950.
35. Xu W., Schluter, O.M., Steiner, P., Czervionke, B.L., Sabatini, B. et al. (2008) Molecular dissociation of the role of PSD-95 in regulating synaptic strength and LTD. *Neuron*, **57**, 248-262.
36. Thies, E., and Mandelkow, E.M. (2007) Missorting of tau in neurons causes degeneration of synapses that can be rescued by the kinase MARK2/Par-1. *J. Neurosci.*, **27**, 2896-2907.
37. Knowles, J.K., Rajadas, J., Nguyen, T.V., Yang, T., LeMieux, M.C. et al. (2009) The p75 neurotrophin receptor promotes amyloid-beta(1-42)-induced neuritic dystrophy in vitro and in vivo. *J. Neurosci.*, **29**, 10627-10637.
38. Nesic, D., Miller, M.C., Quinkert, Z.T., Stein, M., Chait, B.T. et al. (2010) Helicobacter pylori CagA inhibits PAR1-MARK family kinases by mimicking host substrates. *Nature Struc. Mol. Biol.*, **17**, 130-132.
39. Lizcano, J.M., Goransson, O., Toth, R., Deak, M., Morrice, N.A. et al. (2004) LKB1 is a master kinase that activates 13 kinases of the AMPK subfamily, including MARK/PAR-1. *EMBO J.*, **23**, 833-843.

- 1
2
3
4
5
6
7
8
9
10
11
12
13
14
15
16
17
18
19
20
21
22
23
24
25
26
27
28
29
30
31
32
33
34
35
36
37
38
39
40
41
42
43
44
45
46
47
48
49
50
51
52
53
54
55
56
57
58
59
60
40. Hoover, B.R., Reed, M.N., Su, J., Penrod, R.D., Kotilinek, L.A. et al. (2010) Tau mislocalization to dendritic spines mediates synaptic dysfunction independently of neurodegeneration. *Neuron*, **68**, 1067-1081.
41. Ittner, L.M., Ke, Y.D., Delerue, F., Bi, M., Gladbach, A. et al. (2010) Dendritic function of tau mediates amyloid-beta toxicity in Alzheimer's disease mouse models. *Cell*, **142**, 387-397.
42. Matenia, D., and Mandelkow, E.M. (2009) The tau of MARK: a polarized view of the cytoskeleton. *Trend. Biochem. Sci.*, **34**, 332-342.
43. Shankar GM, Bloodgood BL, Townsend M, Walsh DM, Selkoe DJ, et al. (2007) Natural oligomers of the Alzheimer amyloid-beta protein induce reversible synapse loss by modulating an NMDA-type glutamate receptor-dependent signaling pathway. *J. Neurosci.*, **27**, 2866-2875.
44. Hsieh, H., Boehm, J., Sato, C., Iwatsubo, T., Tomita, T. et al. (2006) AMPAR removal underlies Abeta-induced synaptic depression and dendritic spine loss. *Neuron*, **52**, 831-843.
45. Bero, A.W., Yan, P., Roh, J.H., Cirrito, J.R., Stewart, F.R. et al. (2011) Neuronal activity regulates the regional vulnerability to amyloid-beta deposition. *Nat. Neurosci.*, **14**, 750-756.
46. Kamenetz, F., Tomita, T., Hsieh, H., Seabrook, G., Borchelt, D. et al. (2003) APP processing and synaptic function. *Neuron*, **37**, 925-937.
47. Yu, W., Sun, Y., Guo, S., and Lu, B. (2011) The PINK1/Parkin pathway regulates mitochondrial dynamics and function in mammalian hippocampal and dopaminergic neurons. *Hum. Mol. Genet.*, **20**, 3227-3240.

FIGURE LEGENDS

Figure 1. Overexpression of MARK4 causes synaptic and spine abnormality in rat hippocampal neurons. **A-C**, effects of MARK4-WT or MARK4-KD overexpression on postsynaptic PSD-95 clusters (**A**), AMPA receptor GluR1 clusters (**B**), presynaptic Synapsin I clusters (**C**), and spine numbers (**A-C**). Data quantification is shown in **F**. **D**, differential response of PSD-95-S561A and PSD-95-WT synaptic localization to MARK4-WT overexpression. **E**, effect of h-tau-WT or h-tau-S2A co-expression on MARK4-WT overexpression-induced spines loss. **F**, Quantification of spine number and PSD-95 (**A**), GluR1 (**B**), and Synapsin I (**C**) clusters in neurons transfected with MARK4-WT or MARK4-KD ($***P < 0.001$ in Student's *t*-test). **G**, (Left) quantification of PSD-95 clusters in neurons co-transfected with MARK4-WT or MARK4-KD and EGFP-tagged PSD-95-WT or PSD-95-S561A ($***P < 0.001$ in Student's *t*-test). (Right) quantification of spine number in neurons co-transfected with MARK4-WT or MARK4-KD and h-tau-WT or h-tau-S2A ($***P < 0.001$ in Student's *t*-test). Scale bar, 5 μm .

Figure 2. Synaptic and spine toxicity induced by A β oligomers and rescue of A β -induced spine loss by h-tau-S2A. **A**, A β treatment increased endogenous tau phosphorylation at 12E8 sites. Hippocampal neurons at 13 days *in vitro* were treated with A β oligomers for 12 hours and used for western blot analysis. Actin serves as loading control. **B-E**, effects of A β treatment on PSD-95 clusters (**C**), GluR1 clusters (**D**), Synapsin I clusters (**E**), and spine number (**B**) in EGFP-transfected neurons. Data quantification is shown in **B**

1
2
3 (***) $P < 0.001$ in Student's t -test). **F-H**, resistance of h-tau-S2A transfected neurons to
4
5 $A\beta$ -induced loss of spines (**F, G**) and PSD-95 and GluR1 clusters (**H**). Scale bar, 10 μ m.
6
7
8
9

10 **Figure 3.** Inhibition of PAR-1/MARK-mediated tau phosphorylation and MARK4
11 overexpression-induced synaptic and spine toxicity by MKI. **A**, MKI-EGFP inhibited
12 phosphorylation of endogenous tau as assessed by western blot analysis using phosphor-
13 specific antibodies 12E8 and PHF-1 (**A**). **B**, MKI-EGFP inhibited phosphorylation of
14 HA-tagged exogenous h-tau-WT at the 12E8 sites. Robust 12E8 staining (red) is seen in
15 EGFP transfected control neurons. Total tau is stained with anti-HA (blue). **C**, no effect of
16 MKI-EGFP on AMPK kinase activity as detected with the phospho-Acetyl-CoA
17 Carboxylase (Ser79) (pACC) antibody. EGFP transfected neurons serve as control. **D, E**,
18 MKI-EGFP blocked MARK4-overexpression-induced loss of spines (**D, E**) and PSD-95
19 and GluR1 clusters (**E**). Data quantification is shown in **E** (***) $P < 0.001$ in Student's t -
20 test). Scale bar, 10 μ m.
21
22
23
24
25
26
27
28
29
30
31
32
33
34
35
36
37
38

39 **Figure 4.** Rescue of $A\beta$ -induced synaptic and dendritic spine defects by MKI at the
40 morphological and electrophysiological levels. **A-C**, Effects of MKI-EGFP on $A\beta$ -
41 induced loss of PSD-95 (**A**) and GluR1 (**B**) clusters and spine numbers. Neurons
42 transfected with MKI-EGFP or EGFP were treated with $A\beta$ oligomer or mocked treated
43 with solvent as control. The cytoplasmic GFP signals allowed detection of dendritic
44 spines, and PSD-95 or GluR1 clusters were detected by immunostaining. Quantification
45 of data is shown in **C** (***) $P < 0.001$ in Student's t -test). **D**, sample traces of synaptic
46 activity (mEPSCs) recorded in neurons from 4 different conditions (control-EGFP, $A\beta$,
47
48
49
50
51
52
53
54
55
56
57
58
59
60

1
2
3 MKI-EGFP+A β and MKI-EGFP alone) held at -70mV. Summary graphs from 4-6 culture
4
5
6 sets plotting normalized mEPSC frequency and mEPSC amplitude are shown beneath the
7
8
9 traces. Scale bar, 5 μ m.
10
11
12
13
14
15
16
17
18
19
20
21
22
23
24
25
26
27
28
29
30
31
32
33
34
35
36
37
38
39
40
41
42
43
44
45
46
47
48
49
50
51
52
53
54
55
56
57
58
59
60

For Peer Review

ABBREVIATIONS:

A β : amyloid beta

ACC: acetyl-CoA carboxylase

AD: Alzheimer's disease

AMPA: α -amino-3-hydroxy-5-methyl-4-isoxazolepropionic acid

AMPK: AMP activated kinase

AP: amyloid plaque

Dlg: Discs large

GFP: green fluorescent protein

GluR: glutamate receptor

LTD: long-term depression

MARK: microtubule affinity regulating kinase

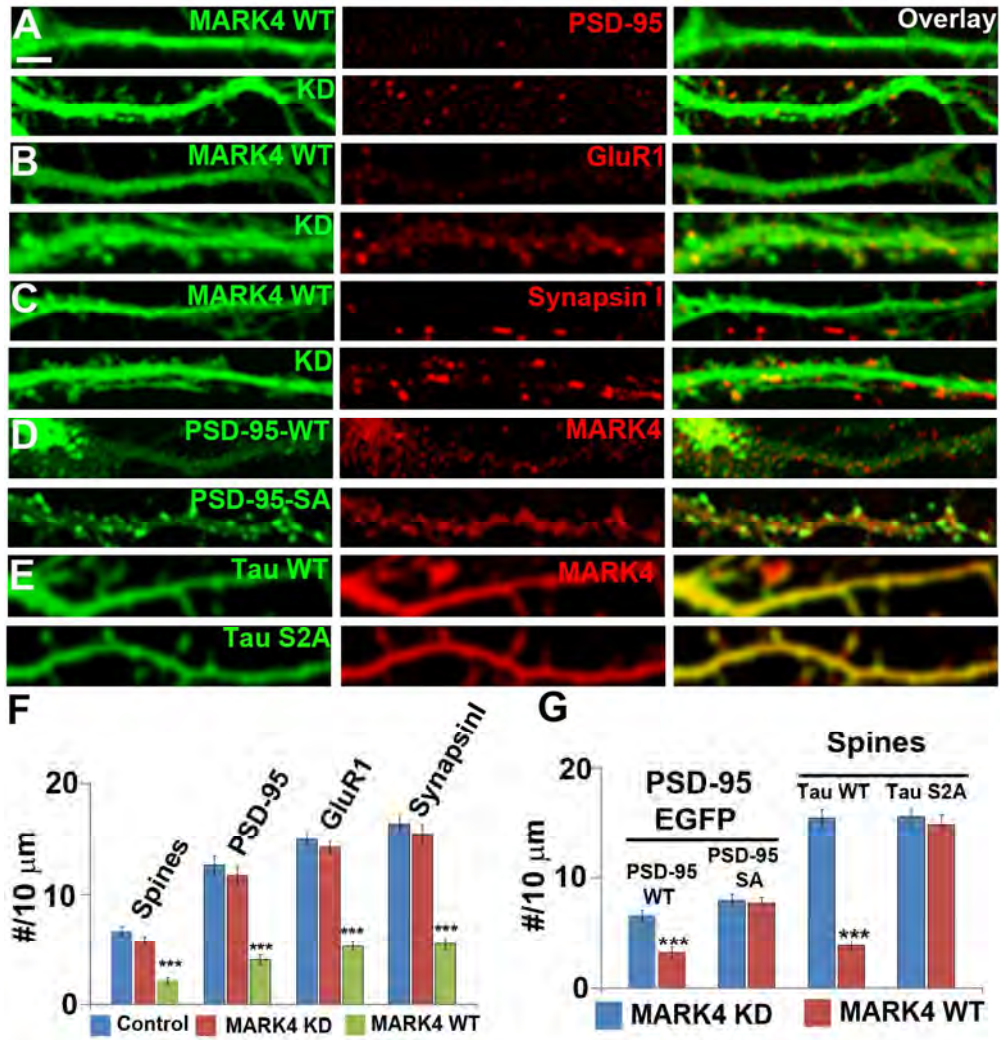
mEPSC: miniature excitatory postsynaptic current

MKI: MARK kinase inhibitor

NFT: neurofibrillary tangle

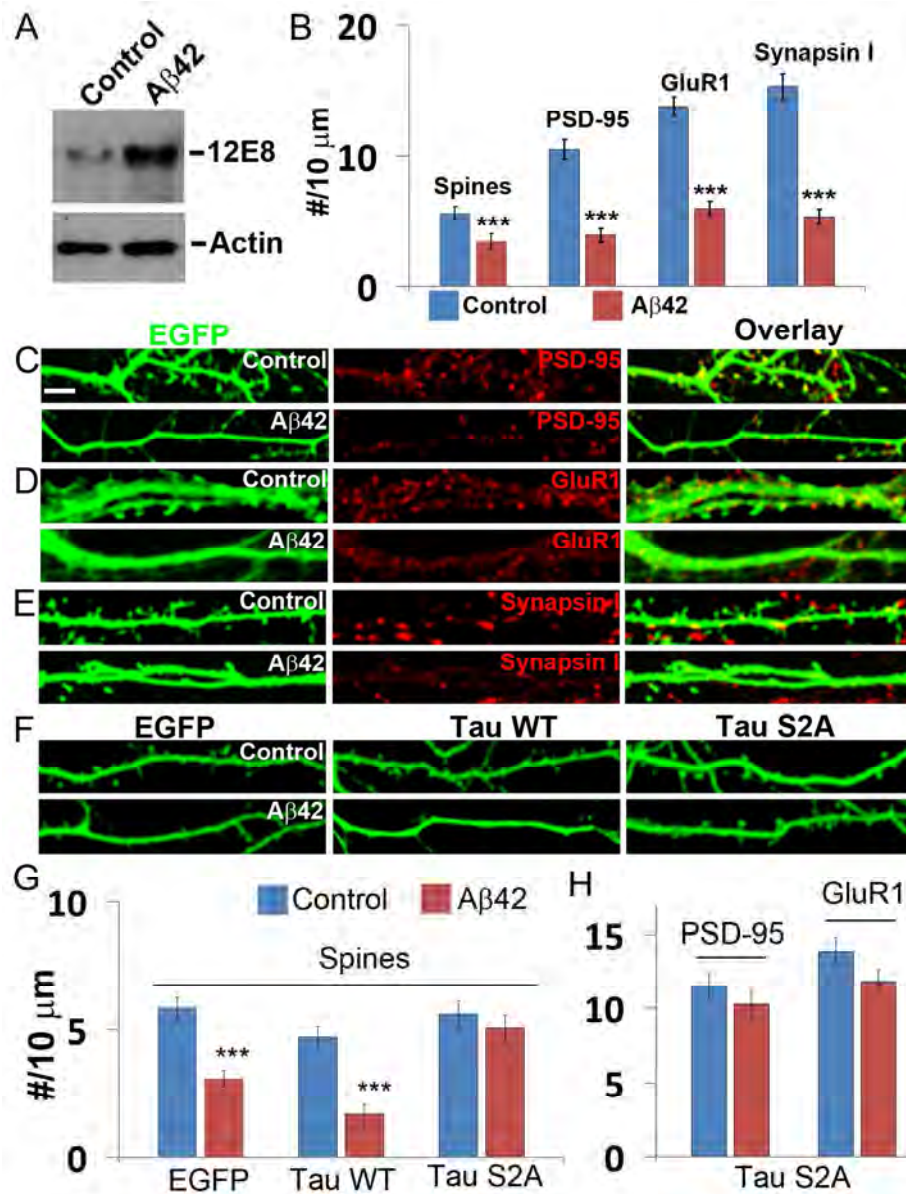
PAR-1: partitioning defective-1

PSD-95: postsynaptic density protein-95



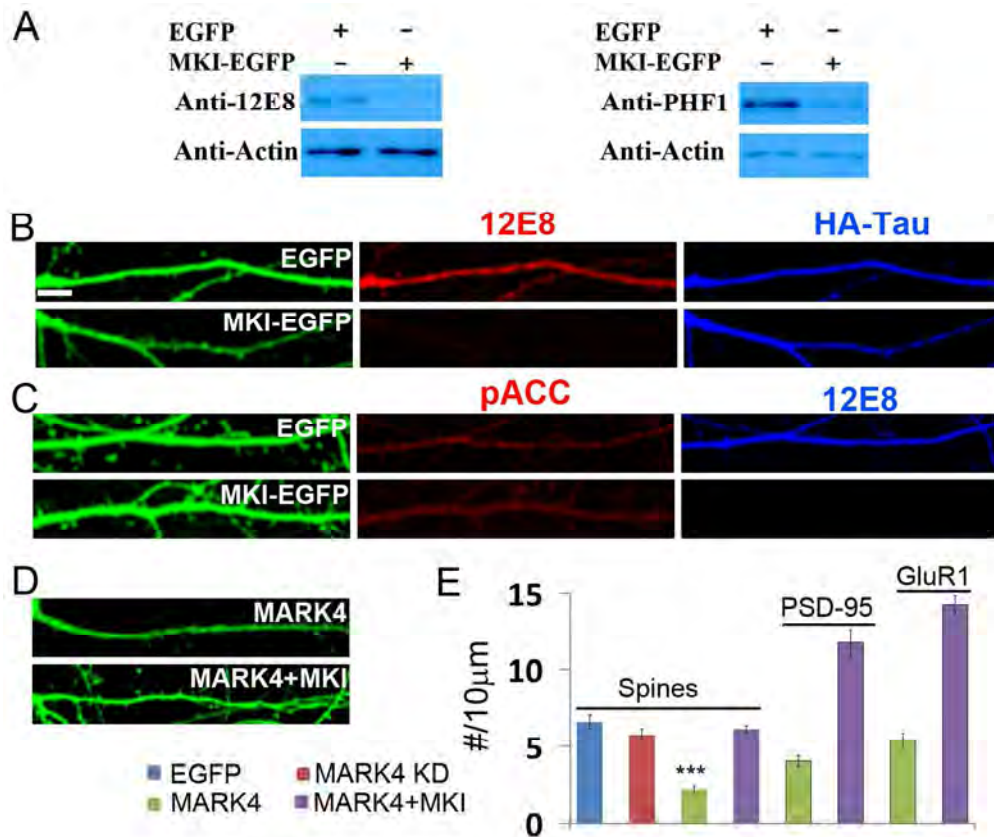
125x131mm (300 x 300 DPI)

1
2
3
4
5
6
7
8
9
10
11
12
13
14
15
16
17
18
19
20
21
22
23
24
25
26
27
28
29
30
31
32
33
34
35
36
37
38
39
40
41
42
43
44
45
46
47
48
49
50
51
52
53
54
55
56
57
58
59
60



130x170mm (300 x 300 DPI)

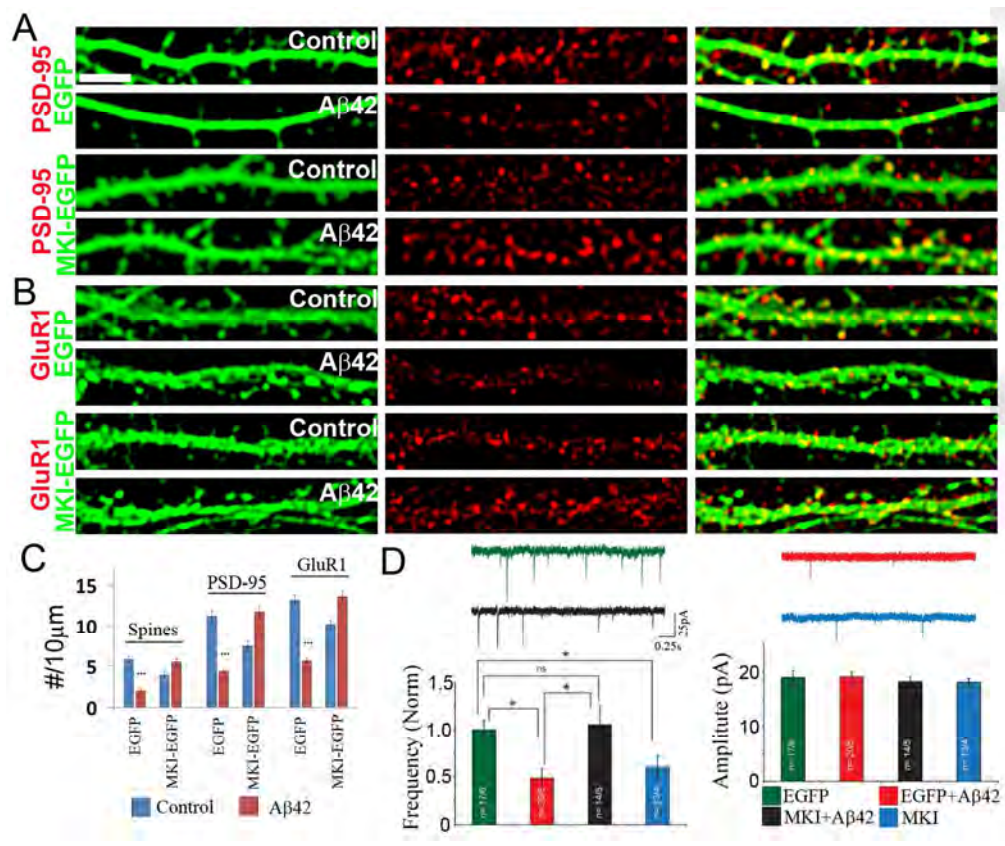
1
2
3
4
5
6
7
8
9
10
11
12
13
14
15
16
17
18
19
20
21
22
23
24
25
26
27
28
29
30
31
32
33
34
35
36
37
38
39
40
41
42
43
44
45
46
47
48
49
50
51
52
53
54
55
56
57
58
59
60



128x107mm (300 x 300 DPI)

view

1
2
3
4
5
6
7
8
9
10
11
12
13
14
15
16
17
18
19
20
21
22
23
24
25
26
27
28
29
30
31
32
33
34
35
36
37
38
39
40
41
42
43
44
45
46
47
48
49
50
51
52
53
54
55
56
57
58
59
60



134x112mm (300 x 300 DPI)

view